Journal of Ocean Engineering and Technology, Vol. 3, No. 2, pp. 587~600, December, 1989

⊙ Technical Paper

Establishment of Fracture Mechanics Fatigue Life Analysis Procedures for Offshore Tubular Joints

Part II : Fatigue Life Analysis for a Multi-Plane Tubular Joint

H. C. Rhee*

(*Received October* 24, 1989)

해양구조물의 원통형 조인트에 대한 파괴역학적 피로수명 산출방법의 설정

제2부 : 두평면 원통형 조인트에 대한 피로수명 분석

李 喜 鍾*

Key Words : Fracture Mechanics(파괴역학), Fatigue Life(피로수명), Wold Toe Surface Crack (용접부위 표면균열), Tubular Joint(원통형 조인트), Stress Intensity Factor(응력확대계수), Crack Instability(균열성장 불안정)

초 록

해양구조물의 원통형 조인트에 대한 파괴역학적 피로수명 산출방법이 개발되었다. 개발된 방법을 이용해서 2평면 K형 조인트에 대한 피로수명을 구체적인 파괴역학적 방법으로 산출하였다. 이 분석을 위해 용접부위 표면균열의 응력확대 계수를 3차원 유한요소법에 의해 계산하였다.

계산된 결과에 의하면 용접부위 표면균열 첨단은 단순한 Mode I형태를 보이지 않고 Mode I, II, III이 복합된 형태임이 입증되었다. 계산된 응력확대 계수를 사용해서 16개의 용접부위 균열 성장형태를 일반적인 피로균열 성장법칙을 적용해서 계산하였고, 균열성장의 안정분석을 통해 각 균열의 최종 파괴상태를 파괴해석도면(failure assessment diagram)법을 이용해서 계산하였다.

1. Introduction

Fracture mechanics has recently become an important part of offshore structural design and integrity assessment. An offshore platform structure is susceptible to defect development during its operation due to corrosion, mechanical damage, fatigue crack initiation, etc. For the safety assessment of an existing offshore structure with crack-like defects, fracture mechanics methods are the most reliable. For such defects in existing structures, the conventional S−N curve procedure is inadequate for fatigue life analyses, and it is inevitable to resort to such methods as fracture mechanics methods for reliable results. Even for design analyses of welded components, the fracture mechanics approach is more reliable than the

* Member, Conoco Inc., U.S.A.

conventional because fatigue lives are dominated by propagation life due to welding induced geometric irregularities and the fracture mechanics method considers the structural conditions more accurately in an analysis than the conventional method.

Fracture mechanics methods require structural data and analysis procedures which are generally more rigorous and expensive to obtain than those for the conventional approach. The complexity of offshore structural conditions make a rigorous implementation of fracture mechanics methods even more difficult. This fact has been one of the major reasons for the delay in the development of the fracture mechanics technology in the offshore industry, compared to the other structural and materials engineering technologies.

One of the most difficult aspects of offshore tubular joint fracture mechanics fatigue life analyses is the calculation of the stress intensity factors because of the geometric complexity of a tubular joint bracechord intersection area. A tubular joint weld toe surface crack is often warped along its surface length following the weld toe contour line along the tubular intersection curve, as well as along its depth. Recently a finite element analysis procedure was developed to calculate the stress intensity factors of such surface flaws. The stress intensity factor solutions of weld toe surface flaws obtained through these methods reveal that, depending on the loading conditions, the crack tip material behavior can be significantly mixed mode. Utilizing these stress intensity factor solutions, detailed fatigue crack growth simulation analyses have been performed to assess the fatigue life of tubular joints. Through these analyses, it has been concluded that such rigorous fracture mechanics analyses are practical, when they are performed using an efficient finite element analysis system.

The objectives of this paper are the development of reliable and systematic fracture mechanics procedures to calculate the fatigue life of an offshore structural tubular joint with defects, and to implement them to a practical tubular joint under realistic environmental fatigue loadings. The model used in the analyses is a multiplane tubular joint common in offshore platforms.

For the reliability of fatigue life calculation for a tubular joint crack, the accuracy of the member force, P, due to offshore environmental loadings, is equivalently important as that of the stress intensity factor, K_I, as apparent from the following Paris crack growth law,

$$da/dN = A(\Delta PK)^m \quad \cdots\cdots(1)$$

where A and m are the material properties, and $K = K_I/P$. In addition to the member force load and stress intensity factor, there are many elements affecting the accuracy of fatigue life analysis results, such as, variable amplitude loading, fatigue crack closure, etc. This sutdy does not intend to deal with all these elements including the fatigue member forces. In the present development of fatigue life analysis procedures, the emphasis is placed on the immediate fracture mechanics aspects, such as, the stress intensity factor and crack instability analysis including some aspects of the welding residual stress.

2. Analysis Procedures

The environmental loads, under which offshore structural components are subjected, are often categorized into two groups for desgin purposes. One is composed of low amplitude cyclic fatigue loads. The other is less frequent design extreme loads, which are generally due to a hundred year storm. Figure 1 shows the behavior of a defect in a stiffened joint under such loading systems.

When a defect in a structural component is subjected to environmental cyclic loadings for an extended duration, it behaves as a crack initiator, from which subcritical fatigue crack propagation starts. The storm loads are infrequent and, thus, do not affect the fatigue crack propagation behavior, but they can be so severe that an instantaneous member failure can be caused from a pro-

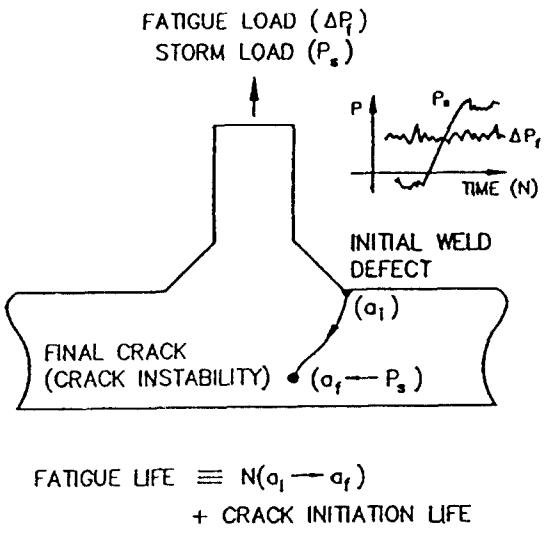

Fig. 1 Fatigue crack growth behavior in welded component

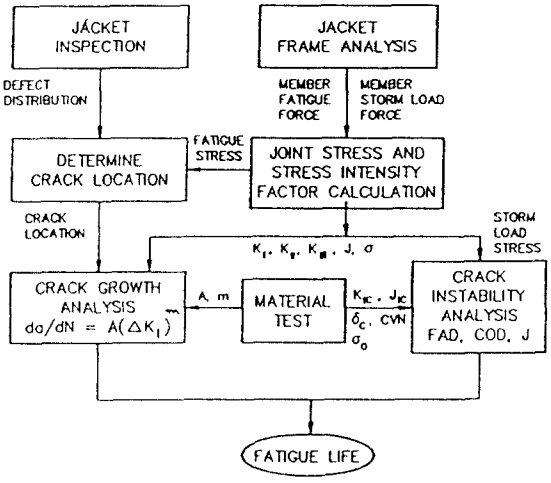

Fig. 2 Fracture mechanics fatigue life analysis procedures

pagating fatigue crack. The fatigue life of a component is the time for a crack to grow from the initial size to the failure size (crack propagation life) plus the time required for the crack initiation.* Therefore, to determine the fatigue life for a crack, it is necessary to perform both fatigue crack growth simulation analysis with the fatigue loads and failure analysis with the design storm loads.

A fatigue crack growth analysis can be performed using a crack growth law, such as the Paris law, for a crack at the most critical location along the brace-chord intersection, which should be determined based on the stress and defect distributions of a tubular joint. For a cracked steel structure, the common mode of failure is either plastic collapse or crack instability (brittle fracture). This failure analysis should also be performed using a fracture mechanics crack instability analysis method, such as the J-integral method[1], the failure assessment diagram method[2),3)], the COD design curve method[4)], etc., because of the crack.

For a fatigue crack growth analysis, the stress intensity factor solutions are required. Depending on analysis method, various different fracture parameters are required for a crack instability analysis. For a J-integral based analysis method, such as the critical load assessment method and the tearing instability theory, the J-integral solutions are required. The failure assessment diagram method uses the stress intensity factors and the plastic collapse loads. The material properties, which are required for fatigue crack growth and crack instability analyses, should be defined consistently with these various fracture parameters.

Figure 2 presents all the ingredients required to complete a fatigue life calculation in a diagram with the appropriate structural properties. Major important steps of fracture mechanics fatigue life calculation procedures are summarized as follows.

1) Calculate fatigue and storm member forces through frame analyses for a jacket under a given environment.

* For a welded component, the initiation life may not be significant, compared to the propagation life, due to the welding induced geometric irregularities.

2) Determine the crack location for fatigue crack growth simulation analyses based on the stress analysis results and defect distribution status.
3) Calculate the stress intensity factors for the fatigue crack growth simulation analyses, and other fracture parameters required for crack instability analyses. Calibrate the material fatigue and fracture properties required consistently with the fracture parameters.
4) Perform fatigue crack growth simulation analyses.
5) Peform crack instability analyses to determine the critical crack size.
6) Correlate the results of the fatigue crack growth and crack instability analyses to determine the component fatigue life.

3. Example Analyses

The geometry and material properties of the analyzed multiplane tubular joint are presented in Figure 3. On the plug of the brace concerned, the clockwise weld toe position is numerically indicated. The structural data used in the analyses are discussed as follows.

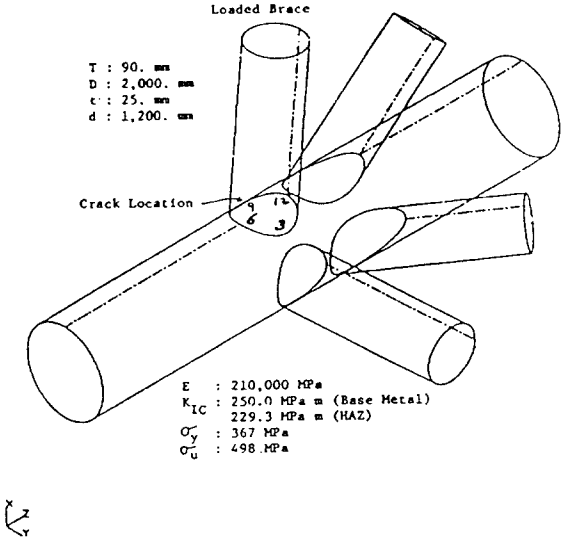

Fig. 3 Multiplane K-joint

3.1 Fatigue and Storm Loads

In the generation of the fatigue load cases, waves with five different heights from eight directions were considered. For the member force calculation, each of these forty waves was applied in six wave positions. The number of load cycles per year for each of the forty loads was calculated from the probability of the corresponding wave in the North Sea. For the storm loads, waves with eight different heights from the eight different directions of a hundred year storm in the North Sea were considered.* The considered loading modes at the end of the concerned brace are axial force, in-plane bending moment, out-of-plane bending moment, and torsion.

3.2 Crack Location

The joint was first analyzed without any crack to obtain stress distributions along the brace-chord intersection under the above mentioned brace forces using a finite element analysis program TUJAP[5]. Figures 4 and 5 show the SCF distributions along the chord side weld toe and through the chord wall at the 9 o'clock position, respectively. The distance along the chord wall

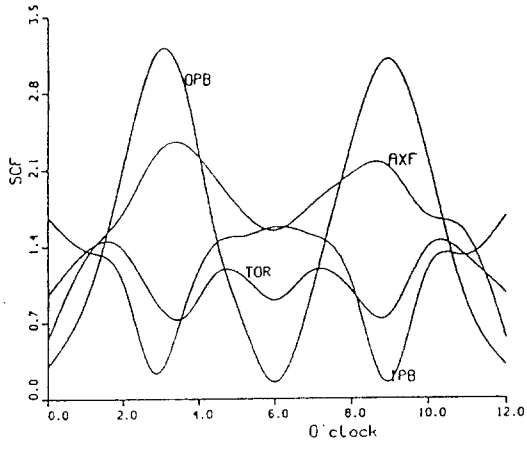

Fig. 4 SCF variation along chord side weld toe

* For details about the fatigue and storm loads, see Reference 14.

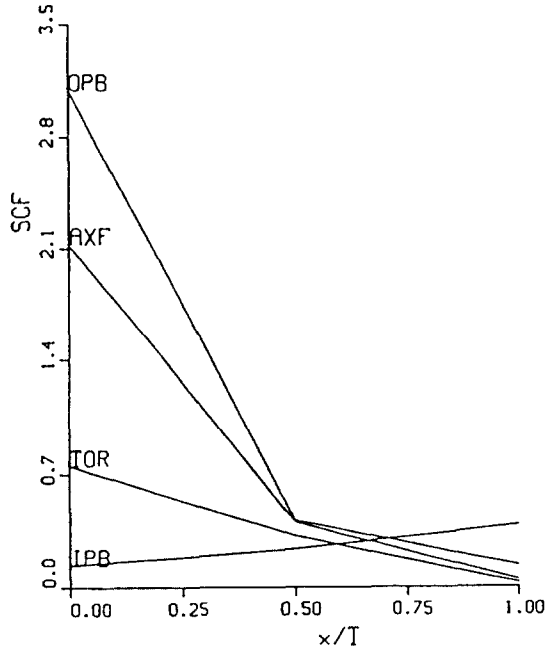

Fig. 5 SCF variation along chord wall thickness

from the outer surface at the 9 o'clock position is denoted by × in Figure 5. Close resemblances in their stress distribution states are observed between the brace axial and in-plane bending loads, and between the out-of-plane bending and torsion loads.

To assess the fatigue stress distribution, the weighted principal stress sum was calculated as

$$\bar{\sigma} = \sum_{i=1}^{40} \left(\sum_{j=1}^{4} \bar{\sigma}_{ij} \right) N_i \Big/ \sum_{k=1}^{40} N_k \quad \cdots\cdots\cdots\cdots (2)$$

where N_i (N_k) is the ith (kth) fatigue load cycle number, and $\bar{\sigma}_{ij}$ (j=1, 2, 3, 4) is the principal stress resulted by one (the jth) of the four brace loads of the ith fatigue load case. The weighted principal stress sum of all four modes of load is highest at the chord side 9 o'clock position. Assuming no defects along the weld toe area, the 9 o' clock position was selected as the crack location.

3.3 Stress Intensity Factor Calculation

A weld toe surface crack was modelled with its length following the chord side weld toe and its depth perpendicular to the chord surface.

This crack was assumed as semielliptical on a flat rectangular plane, which is defined by the weld toe curve and the chord thickness perpendicular to the chord surface. The deepest depth dimension and the half surface length of this crack are represented by a and c, respectively.

The finite element method was used to calculate the stress intensity factors of this crack, which was modelled with the quarter-point crack tip singular elements.[6] Figure 6 shows one of the finite element models used for the stress intensity factor calculation. The models were developed by the preprocessor of TUJAP. Fourteen different cracks (Table 1) were analyzed following procedures of Reference 7.

Figures 7 through 10 show the stress intensity factor distributions along the crack front of one of the fourteen cracks. For all the loading conditions, the mixed mode crack tip material behavior of the crack is clearly demonstrated in these figures. The negative K_I solutions in Figures 7 and 9 indicate that the crack surfaces contacted and penetrated each other during loading. This physically impossible behavior occurred because TUJAP does not have a contact algorithm. The entire stress intensity factor solutions near the area of crack surface penetration should be affected by this physically unreasonable model behavior. However, the effects of possible error resulting from this model behavior may not be significant at the other end of the crack.

The solid dot data plots of Figures 7 through 10 represent the respective effective stress intensity factors, which were developed from the energy release rate expression of a mixed mode problem. For a mixed mode problem, all the existing components of the stress intensity factors contribute to fatigue crack propagation. It is necessary to develop an effective crack driving force parameter to incorporate all the existing stress intensity factors in the fatigue crack growth analysis of a mixed mode problem. Presently, for a fully mixed mode problem, there is no universally ac-

Table 1 Analyzed crack geometries

c/T	0.33	0.86	1.51	3.02
a(*mm*)				
4.5	×			
6.0		×		
9.0	×	×	×	×
36.0	×	×	×	×
67.5	×	×	×	×

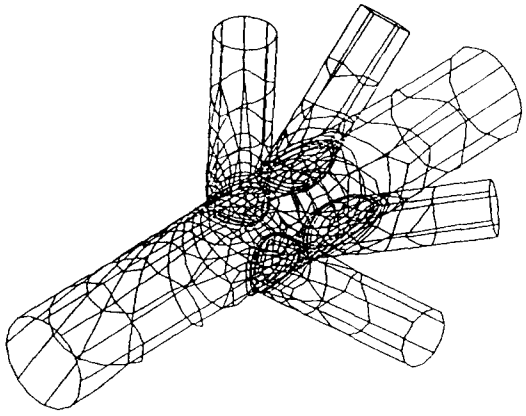

Fig. 6 Finite element model

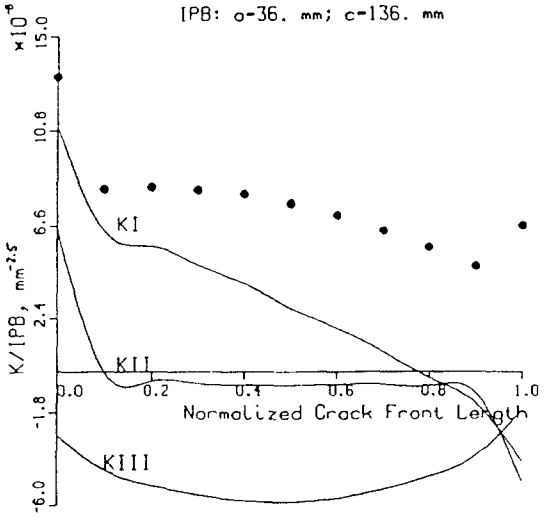

Fig. 7 Stress intensity factors of weld toe surface flaw (In-plane bending)

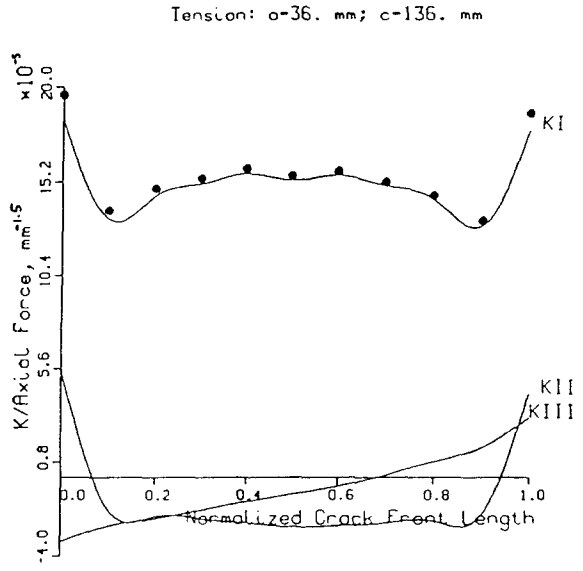

Fig. 8 Stress intensity factors of weld toe surface flaw (Axial tension)

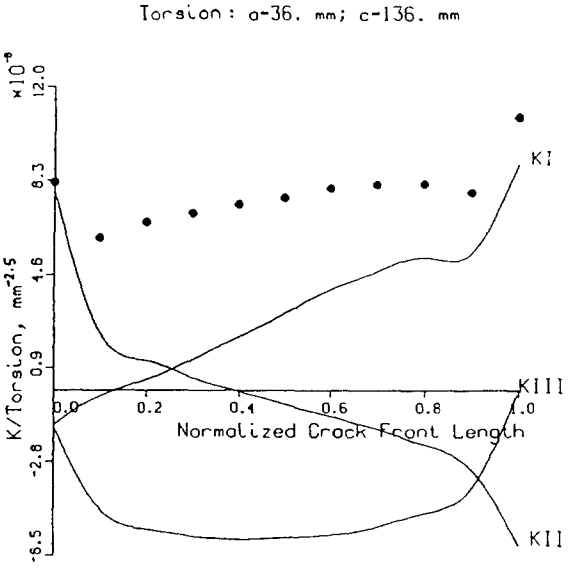

Fig. 9 Stress intensity factors of weld toe surface flaw (Torsion)

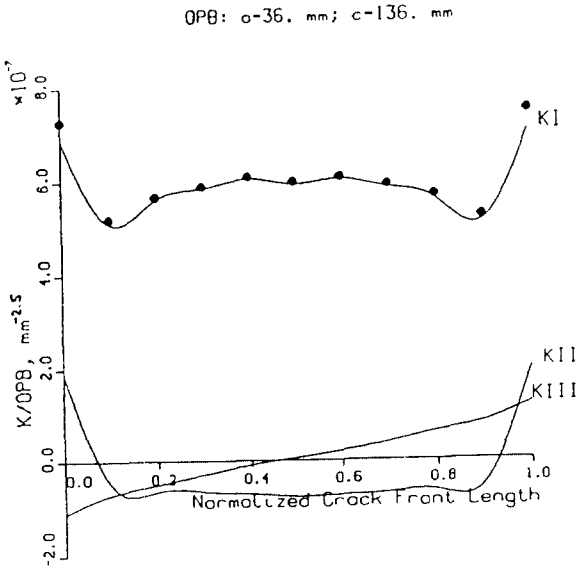

Fig. 10 Stress intensity factors of weld toe surface flaw (Out-of-plane bending)

cepted form of the effective stress intensity factor, which can be used as the crack driving force parameter with a fatigue crack growth law.

For fatigue crack growth analyses, it is necessary to have the stress intensity factor solutions for cracks with various sizes in a range, in which the crack propagation is expected. In the present analyses, for each of the four brace loading modes, the effective stress intensity factors for sixteen different cracks with four depths (a/T = .05, .1, .4, and .75) and four lengths (c/T = .33, 0.86, 1.51, and, 3.02) were first developed from those of the fourteen cracks of Table 1. The cubic polynomial expressions of the effective stress intensity factors at the deepest crack front point and tubular surface crack front point (with the higher stress intensity factors)* were then developed through interpolations of the respective 4× 4 matrices of the effective stress intensity factors in terms of the crack depth and length as discussed later. For three long flaws in Table 1 with depth a/T = 0.05, the stress intensity factor solutions for the depth were extrapolated from those of the larger depths.

3.4 Crack Growth Simulation for Weld Toe Surface Flaw

For fatigue crack growth analyses, the crack growth law developed by Southwest Research Institute[8] for cathodically protected seawater environment under low R-ratio loading was used.

$$\frac{1}{d\ell/dN} = \frac{8\times10^{36}}{\Delta K^{32}} + \frac{2.9\times10^{13}}{\Delta K^{5.93}} - \frac{2.9\times10^{13}}{[(1-R)K_c]^{5.93}} + 10^6 \quad \cdots\cdots (3)$$

where ℓ is the crack size parameter, N is the load cycle number, $d\ell/dN$ is in *m/cycle*, the stress intensity factor range, ΔK is in *MPa* $\sqrt{m}$, the material toughness in stress intensity factor, K_c is 250 *MPa* $\sqrt{m}$, and R is R-ratio. In the analyses, the previously mentioned effective stress intensity factor was used for the stress intensity factor range.

For a weld toe surface flaw fatigue life analysis, a fatigue crack growth simulation poses significant difficulties, in addition to the stress intensity factor calculations. Since the weld toe flaw is two-dimensional, the stress intensity factors depend on the crack shape, as well as, its size. So does the crack propagation behavior. Because the crack growth law is given in a single size parameter, it should be implemented with modification to incorporate the crack shape to the crack growth behavior.

Another difficulty of a surface flaw fatigue analysis is in the fact that a surface flaw has a continuous crack front along which the stress intensity factors vary, and that during crack propagation, the crack front shape continuously changes. It is

* The cracks are not symmetric.

not well understood how the instantaneous stress intensity factor distribution affects the crack front shape change.

It is not practical to model, in an analysis, the arbitrary crack front shape as it is. An idealization of a crack front by an elliptical curve as recommended by the ASME code[9], in conjunction with an assumption in the manner of the crack growth, as follows, can make the problem manageable.

In the analyses, it was assumed that the present effective stress intensity factors at the deepest point, K_a, and at the surface point, K_c, will determine the elliptical shape of the growing crack following the crack growth law, Equation (2). Through integrating Equation (2) with a (or c) for ℓ , and with the instantaneous K_a (or K_c), the increment crack depth (or length) can be calculated.

The stress intensity factor (K_a or K_c) range experienced by a crack under a wave progressively passing in six steps was calculated by following :

$$\Delta K = K_{max} - K_{min} \quad \cdots\cdots\cdots\cdots\cdots\cdots \quad (4a)$$

where K_{max} are respectively the maximum and minimum of the stress intensity factor amplitudes for the wave,

$$K = Pk_1 + OB\ k_2 + IB\ k_3 + T\ k_4 \quad \cdots \quad (4b)$$

with P, OB, IB, and T respectively being the amplitudes of the axial force, out-of-plane bending moment, in-plane bending moment, and torsion. The k_m ($m=1, 2, 3, 4$) associated with these load components represent the respective stress intensity factor per unit magnitude of the corresponding member force.

For each of the four k_m factors, the sixteen associated point values at the deepest (or surface) crack front point for a load case were interpolated in the range of $0.05 \leqq a/T \leqq 0.75$ and $0.33 \leqq c/T \leqq 3.02$ using two-dimensional Lagrange interpolation functions as :

$$k_m = \sum_{i=1}^{4} \sum_{j=1}^{4} K_{ij} L_j M_i \quad \cdots\cdots\cdots\cdots\cdots \quad (5)$$

where K_{ij} ($i,j=1, 2, 3, 4$) are k_m values at $(a/T)_i$ and $(c/T)_j$, and L_j and M_i are the cubic Lagrangean interpolation functions of c/T and a/T, respectively.

4. Crack Instability Analysis

There are considerable difficulties in a crack instability analysis for a cracked tubular joint member. These difficulties originate from its complexities of geometric and loading conditions. These structural complexities can make the crack tip material behavior mixed mode as indicated by the stress intensity factor solutions of Figures 7 through 10. For a fully mixed mode fracture mechanics problem, there is no proven failure criterion. The complex three-dimensional nature in the stress state near the brace-chord intersection area of a tubular joint makes the applicability of any existing engineering approach, such as the COD design curve method, the failure assessment diagram method, the J-integral method, etc., questionable in a rigorous sense. However, if proper judgement is exercised in their applications, reasonable results can be obtained through the utilization of engineering approaches in the fracture mechanics.

In the present analyses, the failure assessment diagram method was used. It is postulated, in the failure assessment diagram method, that a cracked member failure is bounded by two extremes, viz., pure brittle fracture in one end and plastic collapse at the other. The brittle failure parameter is defined by

$$K_r = K_I / K_{IC} \quad \cdots\cdots\cdots\cdots\cdots\cdots \quad (6)$$

where K_I is the Mode I stress intensity factor and K_{IC} is the corresponding plain strain material toughness. The plastic collapse mode parameter is given by

$$S_r = \sigma_1 / \sigma_0 \quad \cdots\cdots\cdots\cdots\cdots\cdots \quad (7)$$

where σ_1 is the applied stress contributing to plastic collapse, and σ_0 is the plastic collapse stress

for the component. When the location of the point defined by (S_r, K_r) is outside of the failure assessment curve in a failure assessment diagram (FAD), the member is unsafe. A FAD is developed in a two-dimensional rectangular coordinate plane with S_r and K_r as its coordinates. The original R6 failure assessment curve[2] was derived using the plain strain crack opening displacement expression of the Dugdale strip yield model[10]. Later on the failure assessment curve was modified by various investigators to incorporate material hardening behavior, ductile tearing of a crack, crack size effects, etc. In the present analyses, the original R6 curve and curves developed for nuclear reactor vessel class steel materials[3] were used as reference failure assessment curves.

Among the sixty four storm load cases, the critical storm load case selected was the one which developed the maximum effective stress intensity factors at the deepest and weld toe surface crack front points of a crack. For all the cracks during the fatigue crack propagation, it was found that Load Case 8 was the critical one. For this critical storm load case, the effective stress intensity factor and the applied stress contributing to plastic collapse were calculated following procedures discussed below.

For the brittle fracture parameter, K_r, all the existing local stresses consisting of those due to four brace forces and welding residual stresses will make contributions. To include the welding residual stress effects, the effective stress intensity factor resulted by a brace axial tension, which makes the hot spot (9 o'clock position) yield, were added to that of the critical storm loads. Since the welding residual stress is a self-equilibrating stress system, the stress distribution due to the brace tension is considered to be a conservative approximation for the residual stress. This is apparent from Figure 5.

To include the plastically adjusted crack length effects, the effective stress intensity factor, K_e, with the combined storm load and the welding residual stresses was modified to obtain the plastically adjusted stress intensity factor, K, which represents K_a or K_c, depending on the location on the crack front, as

$$K = K_e \sqrt{\ell_e / \ell} \quad \cdots\cdots (8)$$

where ℓ is the crack size parameter (a or c), the plastically adjusted crack size, ℓ_e is

$$\ell_e = \frac{1}{6\pi} (K_e / \sigma_{ys})^2 + \ell \quad \cdots\cdots (9)$$

The K_r parameter of Equation (6) was obtained by replacing K_I with the above K.

It is unlikely for an existing offshore structure that such a parameter as K_{IC} for Equation (6) is available, since fracture mechanics methods have rarely been utilized in the design and fabrication of conventional offshore structures. Although it is not ideal as a fracture mechanics parameter, the Charpy energy (CVN) can be a practical choice as a material toughness parameter for a crack instability analysis, since it is available for most existing offshore structures.

Two common difficulties in using CVN as a fracture mechanics toughness parameter for an existing structure are its availability and conversion to a relevant fracture mechanics toughness parameter, such as K_{IC} or CTOD. For the base materials of tubular joints, it is comparatively easy to obtain a proper CVN value, since CVN has been used as a quality control parameter for a long time. However, the reliable HAZ CVN of a joint is not always easy to obtain.

Although many conversion formulas between CVN and K_{IC} are available, there are significant uncertainties in implementing them to a specific case, since, as empirical formulas, they are all based on a specified set of conditions under which the conversion data were generated. In the present analyses, the following formula[11] was used to convert CVN to K_{IC} for both HAZ and base plate material :

$$K_{IC} = 0.22E(CVN)^{1.5} \quad \cdots\cdots (10)$$

where K_{IC} is in $kPa\sqrt{m}$ and CVN is in *joule*.

In the calculation of the plastic collapse load,

the welding residual stress was not considered. Being a self-equilibrating force system, the welding residual stress does not contribute to the section collapse. To calculate the plastic collapse stress due to the critical storm loads, the local principal stresses due to the four brace forces were first algebraically added at three points along the chord thicknes at the 9 o'clock position. These three points are outer, middle, and inner wall surface points and the SCFs on them are shown in Figure 5 for the four brace forces. The resulting principal stress sums at the three points, which were based on the joint without a crack, were fitted into a quadratic curve with respect to the chord thickness. The plastic collapse load at the deepest crack front point (or at the tubular surface crack front point) was then calculated by normalizing the area under this curve by the uncracked ligament length (or by the wall thickness) of a fatigue crack to be analyzed.

The above described plastic collapse load parameter at the deepest crack front point is nothing but the magnitude of the storm load stress to be uniformly distributed on the cross section of the chord wall reduced due to crack growth. In this model, the elliptical shape of the crack surface is approximated by a continuous flaw with a depth identical to that of the deepest point of the actual elliptical crack front. Therefore, the plastic collapse storm load is highly conservative. The average of the yield and tensile strength of the material was used as the plastic collapse stress of Equation (7).

5. Results and Discussions

5.1 Fatigue Crack Growth Analysis Results

Sixteen different cracks were analyzed following the procedures discussed above. For these analyses, the fatigue loads of a year were incrementally applied in twelve equally divided segments. For each segment loading, the forth load cases were applied consecutively following the load case number. During each application of the forty load cases in an increment, the stress intensity range was kept constant. At the end of each load case application, the crack size was updated with the relevant growth in depth and length, and the stress intensity range was recalculated for the new crack size for the next load case application.

The results of the analyses are listed in Table 2. The initial crack geometries were selected to cover a wide range of crack geometries. Especially, those with depth and length equal to or larger than 6 and 140*mm*, respectively, are considered to be highly unlikely as initial welding induced defects for fatigue crack propagation. Except for these extremely large initial defects, all took more than twenty years for seventy five percent wall penetration.

At seventy five percent wall penetration, the final surface lengths of the sixteen cracks were almost identical and were only around thirteen percent of the total circumferential length of the weld toe. It is considered that, even after complete wall penetration of a fatigue crack, with the crack shape extrapolated from this final shape, the joint compliance is unlikely to change significantly and its static strength capability will not be reduced considerably.

Figure 11 shows the fatigue crack depth growth records with the number of years of platform operation. From this plot, it is apparent that most of the crack growth trends to occur in a similar pattern through which extrapolation of crack depth growth can be possible beyond the plotted points. An identical trend to this was observed for the crack length growth plot, which is not presented in this paper. Figure 12 shows the crack shape change during the fatigue crack propagation. Figure 12 indicates that regardless of their initial dimensions, the weld toe surface cracks have a tendency to converge to a single shape, while they are propagating under the considered fatigue loadings. After the convergence, the cracks followed a single growing path to reach an identical crack shape at seventy five percent wall penetration. This trend is consistent with previous

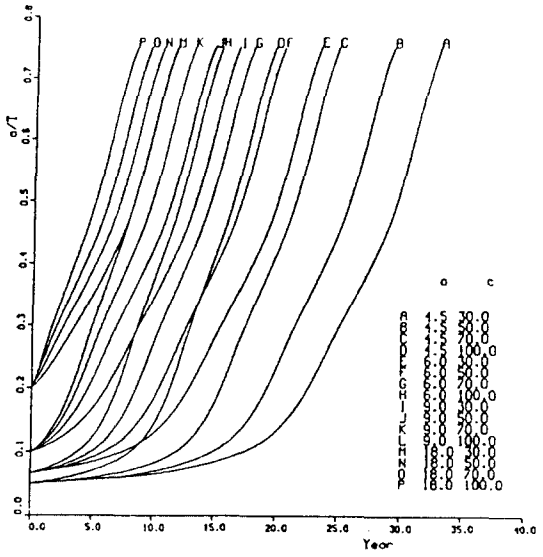

Fig. 11 Fatigue crack growth record

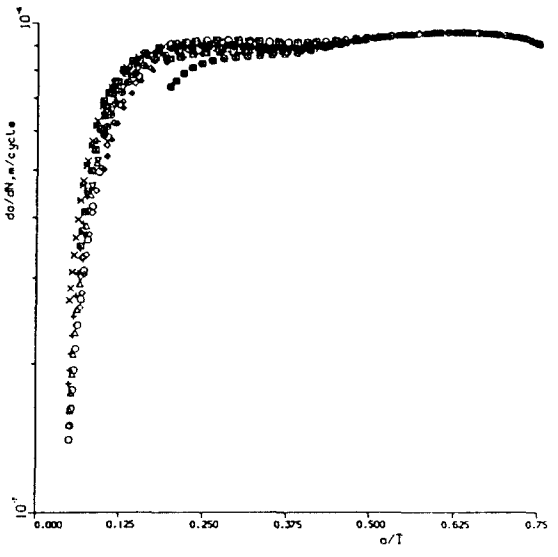

Fig. 13 Crack growth rate

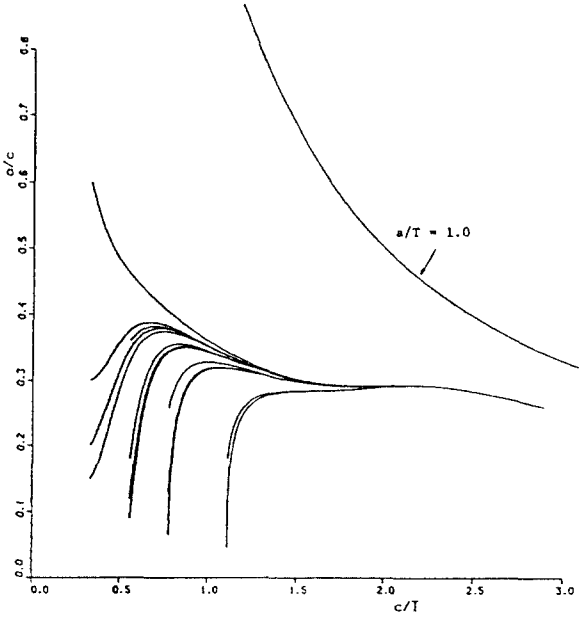

Fig. 12 Crack shape change record (a/c vs. c/T)

analysis results on an X-joint under brace tension loading[12] and on a K-joint under fatigue load typical at the North Sea[13].

Figure 13 shows the crack growth rate changes with crack depth. In the development of these plots, one of the forty fatigue loading cases was used. The initially different crack growth rate curves for cracks with different initial sizes and shapes converge to a single curve as the cracks grow. The crack growth rates vary with the dimensions of the propagating cracks. This form of constant or decreasing crack growth rate trend with fatigue crack extension, which reflects the decreasing stress distribution patterns along the crack growing path, is consistent with that has been observed in many laboratory tests.

5.2 Crack Instability Analysis Results.

The FAD analysis result plot for a selected crack from Table 2 is presented in Figure 14. Two different sets of solutions, viz., with (solid symbols) and without (open symbols) consideration of the welding residual stresses, are presented in this figure. The circular and rectangular symbols represent the data at the deepest and tubular surface crack front points, respectively. For the base material, CVN=175.7 *J*, which can be possible for a BS4360 50D grade steel, was used. For the HAZ, CVN = 109.0 *J* was selected. However, the maximum K_{IC}'s converted from these CVN's were limited to 250.0 $MPa\sqrt{m}$.

As the fatigue cracks grow, the status points

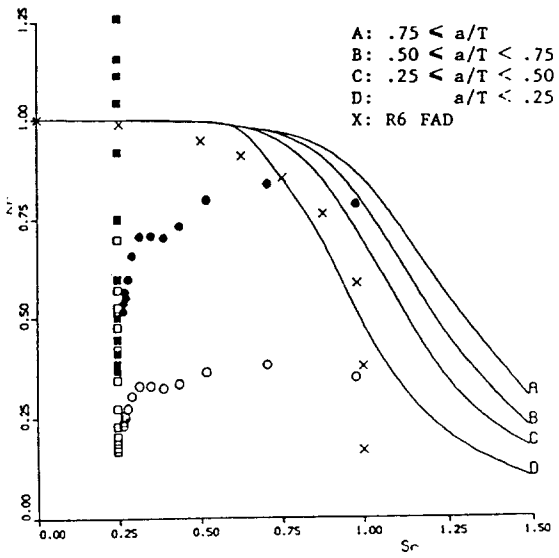

Fig. 14 Failure assessment diagram (a×c = 6×70 *mm*)

move from left to right and from down to up for the deepest and surface crack front points, respectively, in Figure 14. At the later stage of the crack propagation, the deepest and surface crack front points are in the unsafe zone for both cracks, when the welding residual stresses were considered.

Table 2 shows the crack instability fatigue lives of the analyzed cracks. The crack instability life of a crack is the time when the status point of the crack moves outside of the proper failure assessment curve. For all cracks, the first unsafe status developed at the weld toe surface crack front point rather than the deepest crack front point. As indicated from Figure 14, at the surface crack front point, the danger of brittle fracture is more significant than for plastic collapse. This is due to the low material toughness at this point.

The differences between the seventy five percent wall penetration and crack instability lives is significant. This difference increases with the initial crack dimensions and is more sensitive to the initial depth than length. Whether the crack instability on the surface crack front point is practical (and, thus, the crack instability life is credible) or not is a matter of engineering judgement for a specific problem.

Table 2 Fatigue life weld toe crack

Initial crack		Number of years 75% Wall penetration	Crack instability	Final crack	
a, *mm*	2c, *mm*			a, *mm*	2c, *mm*
4.5	60	32.9	26.9	67.5	520.0
	100	29.1	22.4		520.4
	140	24.7	18.9		518.8
	200	19.6	14.9		519.2
6.0	60	23.3	16.9	67.5	521.2
	100	20.3	13.9		517.2
	140	17.8	11.9		520.0
	200	15.2	10.4		518.8
9.0	60	16.6	9.7	67.5	519.8
	100	14.6	7.9		516.4
	140	13.0	6.9		518.4
	200	11.5	6.4		520.0
18.0	60	11.6	4.4	67.5	517.4
	100	10.4	3.4		517.8
	140	9.4	2.9		518.0
	200	8.2	2.9		518.0

6. Conclusions

This paper presented a fracture mechanics analysis procedure for the fatigue life analysis of an offshore tubular joint. Using a multiplane tubular joint, the applicability of this procedure was demonstrated. From this study, the following conclusions can be drawn :

1) For an in-service safety assessment of an existing offshore structure, rigorous fracture mechanics analyses are practical.
2) For most full scale offshore tubular joints, all the data required for the present analyses can be developed with about one hour of CPU time for a recent CRAY machine, when an efficient general purpose finite element program is used.
3) Considering the benefits that can be achieved from such analyses, the computer time requirement, which can be further reduced with new machine developments, is a small investment.
4) For a fracture mechanics fatigue life calculation for an offshore structural tubular joint, it is essential to develop the stress intensity factors appropriate for the specific joint geometry. For this purpose, a numerical method, such as the finite element method, is the only practical approach.
5) It is also essential for such an analysis to develop the material fracture properties consistently with the analysis formulations.

Acknowledgement

The author is grateful to the Conoco management for allowing this publication.

References

1) Rhee, H. C., "Application of the Critical Load Assessment Method for Stable Crack Growth Analysis", Engineering Fracture Mechanics, Vol. 24, No. 6, 1986
2) Harrison, R. P., K. Loosemore, and I., Milne, "Assessment of the Integrity of Structures Containing Defects", CEGB Report No. R/H/6, Central Electricity Generating Board. U. K., 1976
3) Bloom, J. M., "A Procedure for the Assessment of the Structural Integrity of Nuclear Pressure Vessels", Jnl. of Pressure Vessel Technology, Trans., ASME, Vol. 105, February 1983
4) PD6493, "Guidance on Some Methods for the Derivation of Acceptance Levels for Defects in Fusion Welded Joints", British Standard Institution, 1980
5) TUSTRA, "Tubular Joint Structural Analysis Module", User's Manual, RN 83-6150, Veritec, Oslo, Norway, May, 1985
6) Barsoum, R. S., "On the Use of Isoparametric Finite Elements in Linear Fracture Mechanics", Int. Jnl. for Num. Meth. in Engng., Vol. 10, 1976
7) Rhee, H. C., and M. M. Salama, "Mixed-Mode Stress Intensity Factor Solutions for Offshore Structural Tubular Joints by Three-Dimensional Finite Element Analysis", 19th National Symposium on Fracture Mechanics, ASTM, San Antonio, Texas, June 1986
8) Burnside, O. H., S. J. Hudak, Jr., E. Oelkers, K. Chan, and R. J. Dexter, "Long Term Corrosion Fatigue of Welded Marine Steels", Final Report, SwRI Project No. 06-6292
9) ASME Boiler and Pressure Vessel Code, Section XI, "Rules for In-Service Inspection of Nuclear Power Plant Components", ASME, 1977
10) Bilby, B. A., A. H. Cottrell, and K. H. Sowinden, "The Spread of Plastic Yield from a Notch", Proceedings of the Royal Society A272, 1963
11) Rolfe, S. T., and S. R. Novak, "Slow-Bend K. Testing of Medium Strength, High-Toughness Steels", ASTM STP 463, American society for Testing and Materials, 1970
12) Rhee, H. C., "Fatigue Crack Growth Analysis of Offshore Structural Tubular Joint", to Ap-

pear in Engineering Fracture Mechanics.
13) Rhee, H. C., and J. A. Tyson, "Fatigue Life Calculation for Offshore Structural Tubular Joint Using Fracture Mechanics Crack Growth Analysis", OTC 5557, Offshore Technology Conference, Houston, Texas, April, 1987

★뉴 스★

■국제학술대회참가안내■

제9회 국제열전달 학술대회
-Ninth International Heat Transfer Conference-

주 관 : 국제열전달 학술회의(IHTC)
분 야 : 전도, 강제, 자연 및 혼합열전달, 복사, 복합열 및 물질전달, 연소, 융해 및 응고, 비등 및 응축, 이상유동, 계면현상, 분체 및 다공성 매질, 측정기술, 전달성질, 열교환기, 열전달증진, 프로세스 기기, 태양열 원자로 시스템, 전자시스템, 생물공학, 회전기계, 열에너지 저장, 모델링 및 수치기법 등의 연전달의 기초 및 응용분야
일 시 : 1990년 8월 19일~24일(6일간)
장 소 : 이스라엘 예루살렘

※ 기타 자세한 내용은 서울대학교 공과대학 기계공학과 강신형 교수(열 및 유체역학부문위원회 간사)께 문의 바람〔전화번호 (02)886-0101(交)3471〕

제9회 국제 실험 역학회 학술대회
-9th International Conference on Experimental Mechanics-

주 관 : 미국 실험 역학회(SEM), 덴마크 공과대학, Imeko 실험 역학회
분 야 : 실험 역학에 관한 전 분야
(구조물 시험, 광학적인 방법, 재료시험, 파괴역학, 피로시험, 복합재료, 비선형 방법, 생체역학, 스트레인게이지, 잔류응력, 광탄소성, 열응력, 실험역학에의 컴퓨터 응용, 영상 프로세스, 고온특성, AE, 초음파 탐상, 짧은 균열, 동역학 등)
일 시 : 1990년 8월 20~24일(5일간)
장 소 : 덴마크 공과대학(코펜하겐)
일 정 : 1990년 4월 1일 : 논문제출 마감
1990년 5월 1일 : 논문채택 최종 통보

※ 기타 상세한 내용은 인하대학교 공과대학 기계공학과 이억섭 교수께 문의바람.
전화번호 : (032) 862-0077 (교) 2069